Clays and Clay Minerals, Vol. 42, No. 6, 657–666, 1994.

NATURE AND STABILITY OF RADIATION-INDUCED DEFECTS IN NATURAL KAOLINITES: NEW RESULTS AND A REAPPRAISAL OF PUBLISHED WORKS

BLANDINE CLOZEL,[1,*] THIERRY ALLARD,[1] AND JEAN-PIERRE MULLER[1,2]

[1] Laboratoire de Minéralogie-Cristallographie, UA CNRS 09 Universités Paris 6 et 7
4 Place Jussieu, 75252 Paris Cedex 05, France

[2] O.R.S.T.O.M., Département T.O.A., 75480 Paris Cedex 10, France

Abstract—A new appraisal of radiation-induced defects (RID) in natural kaolinite, i.e., positive trapped holes on oxygen atoms, has been undertaken using Q-band EPR spectra, recorded at 93 K, of irradiated annealed and oriented kaolinite samples originating from various environments. Three different centers were identified. Two of the centers, A- and A′-centers, are trapped holes on oxygen from Si-O bonds. They have a distinct signature and orthogonal orientation, i.e., perpendicular and parallel to the (ab) plane, respectively. The third center, the B-center, is a hole trapped on the oxygen bonding Al in adjacent octahedral positions (Al_{VI}-O^--Al_{VI} bridge). This confirmed some previous assignments from the literature, some others are no longer considered as valid.

A least squares fitting procedure is proposed to assess the RID concentration in any kaolinite. It allows a quantitative approach of the thermal stability of RID. Isochronal annealing shows that the thermal stability of the centers decreases in the order A, A′, B over the temperature range 0–450°C: (1) B-center is completely annealed above 300°C; (2) A′-center can be annealed by heating at 400°C for more than two hours; (3) A-center is stable up to 450°C. The activation energy and the magnitude of the mean half-life for A-center is evaluated through isothermal annealing at 350, 375 and 400°C, with E_a = 2.0 eV ± 0.2, and $t_{1/2} > 10^{12}$ years at 300 K. The stability of A-center seems to decrease with increasing crystalline disorder. Nevertheless, it is high enough for radiation dosimetry using kaolinites from any environment on the Earth's surface.

Key Words—EPR, Kaolinite, Radiation induced defects, RID.

INTRODUCTION

Kaolinite, a ubiquitous clay mineral at the Earth's surface (Murray 1988), is known to incorporate stacking defects of various types (e.g., Cases *et al* 1982; Giese 1988). At the layer scale, some point defects may be directly studied through their paramagnetic character, by using Electron Paramagnetic Resonance (EPR). They are trace elements (substituted Fe^{3+}, sorbed Mn^{2+} and VO^{2+} ions) together with defect centers (e.g., reviews by Hall 1980; Pinnavaia 1981; Muller and Calas 1993). Defect centers are detected in all natural kaolinites (Meads and Malden 1975; Muller and Calas 1993). They have been interpreted as positive holes trapped on oxygen atoms, stabilized by diamagnetic precursors (Angel *et al* 1974; Meads and Malden 1975; Cuttler 1980). These hole centers have been demonstrated to be radiation-induced defects (RID), through irradiation experiments and studies of various natural alteration systems (Angel *et al* 1974; Clozel 1991; Muller *et al* 1990, 1992).

RID in kaolinite have been used as fingerprints of the condition of formation and evolution of various kaolinite-containing environments at the Earth's surface (Muller and Calas 1993). In particular, the use of kaolinite as an *"in situ* dosimeter" was proposed, as a unique tool for indirect assessment of radionuclide migration in the geosphere (Muller *et al* 1990, 1992; Ildefonse *et al* 1990, 1991). This implies, however, that the types of RID present in any kaolinite and the parameters which govern their formation and their stability are defined accurately.

The nature and stability of RID are controversial or undefined in some cases, mainly because of lack of relevant EPR-data. In this work, the systematic use of X-/Q-band hyperfrequencies at room/low temperatures, on powder/oriented, and irradiated/annealed samples, allowed: (1) an unequivocal assignment of RID spectra, (2) the quantification of the respective contents of RID in natural kaolinites and (3) the estimation of their geologic time scale stability in environments at the Earth's surface.

MATERIALS AND METHODS

Samples

Six reference kaolinites have been selected among numerous kaolinites from hydrothermal alteration zones, sediments, and soils which were previously investigated with EPR (Clozel 1991; Muller and Calas 1993). Table 1 lists the sources and references for the raw samples, together with disorder indices (obtained from Fourier Transform Infrared Spectrometry (DIR

* Present address: BRGM, DRIGGP, Research Division, Geotechnical Engineering and Mineral Technology, Avenue de Concyr. B.P. 6009, 45060 Orleans Cedex 2, France.

Table 1. Characterization of the samples.

Sample	Source	Reference	Mineralogy[1]	Crystalline order/disorder[2] R2 (DRX)	Crystalline order/disorder[2] DIR (FTIR)	EPR (structural Fe^{3+}, a.u.)[3] Fe(I)	EPR (structural Fe^{3+}, a.u.)[3] Fe(II)	EPR (RID content, a.u.)[4] A	EPR (RID content, a.u.)[4] A'	EPR (RID content, a.u.)[4] B
GB1	St Austell (GB)	Cases *et al* 1982	I ≈ 5%, Q ≈ 5%	1.12	1.01	9	270	4.9	3.4	3.3
GB3	St Austell (GB)	Cases *et al* 1982	I ≈ 10%, Q ≈ 5%	1.08	0.93	6	190	6.0	2.8	2.5
A1	Nopal (Mexico)	Muller *et al* 1990	UBM < 1%	1.18	0.96	3	39	21.1	37.0	3.6
C3	Nopal (Mexico)	Muller *et al* 1990	UBM < 1%	1.03	0.91	16	167	16.0	115.0	10.8
C14	Nopal (Mexico)	Muller *et al* 1990	UBM < 1% h?	1.1	0.87	17	230	13.0	48.0	5.4
BAR (CBD, 1–2 μm)	Gironde (France)	This work	I 15–20%	0.85	1.06	52	600	1.9	0.5	0.9

[1] I = Illite or Muscovite; Q = quartz; UBM = Uranium-bearing minerals; h = halloysite, as determined from XRD and chemical analysis by normative reconstitution (see the respective references).
[2] See definition of crystalline-disorder indices in "Methods" section.
[3] Measured according to the simplified procedure of Mestdagh *et al* 1980.
[4] Measured at 93 K, according to the spectrum decomposition procedure (this paper).

index) and X-ray Diffraction (R2 index, see below), some EPR characteristics (substituted iron and RID content), and pretreatment (deferrification, granulometry). They consist of:

(1) two hydrothermal kaolinites from Cornwall (England), namely GB3 and GB1. They are well-ordered kaolinites, as shown by their disorder indices R2 and DIR, and are associated with minor quartz and muscovite (Cases *et al* 1982).

(2) three hydrothermal kaolinites, A1, C3, and C14 originating from an altered volcanic tuff (Nopal 1 uranium deposit, Chihuahua, Mexico; Ildefonse *et al* 1990), characterized by a low impurity content (substituted iron, ancillary phases as uranium-bearing minerals), a high crystalline order, and a high RID spectrum intensity (Muller *et al* 1990; Ildefonse *et al* 1991).

(3) a sedimentary kaolinite, named BAR, sampled in the Tertiary sedimentary basin in Charentes (France). It has a low crystalline order and a relatively high content of impurities, i.e., substituted iron, associated iron oxides and illite (This study). It was verified that the presence of accessory minerals (illite, weeksite, quartz) was not a limitation to RID identification because of undetectable or readily differentiated contributions in the RID region of the EPR spectra.

Methods

Characterization of samples. X-ray powder diffraction (XRD) data were obtained with a PW 1710 vertical goniometer using monochromatic CuKα radiation (40 kV, 30 mA) at scanning rates of 1°2θ/min. The structural order of the kaolinites was approached using the R2 index of Liétard (1977), which is related to the translations in the (ab) plane. It measures the relative intensity of the (131) and ($1\bar{3}1$) diffraction peaks, according to the relation:

$$R2 = \frac{\frac{1}{2}(I_{(131)} + I_{(1\bar{3}1)}) - k}{\frac{1}{3}(I_{(131)} + I_{(1\bar{3}1)} + k)} \quad (1)$$

where k stands for the local minimum in the (131)/($1\bar{3}1$) inter-peak region.

The crystalline order of the kaolinite samples was also estimated by means of infrared spectroscopy using a Fourier-Transform Infrared (FTIR) Nicolet 5DX spectrometer. The relative intensity of the OH-stretching bands at 3669 and 3649 cm^{-1} is correlated with crystal ordering of kaolinite (Liétard 1977; Cases *et al* 1982; Muller and Bocquier 1987). This index, DIR, is defined as the ratio of the apparent absorbances

$$DIR = [I(3649)/I(3669)] \quad (2)$$

It increases with decreasing crystalline order of kaolinite.

Irradiation experiments. X-ray irradiations were performed to enhance the signal of B centers, according to the observations of Angel *et al* (1974). Samples were annealed thermally at 400°C for 24 hours prior to ar-

https://doi.org/10.1346/CCMN.1994.0420601 Published online by Cambridge University Press

tificial irradiation (see below) in order to destroy most of the defect centers present in natural kaolinites (Angel *et al* 1974; Clozel 1991). The pre-annealed kaolinites were then exposed to X-ray radiation (MoKα source, 35 mA, 50 kV) for 48 h prior to the EPR analysis. Irradiations were performed on kaolinite powders set between kapton sheets close to the X-ray shutter.

Annealing experiments. In previous work, step-annealing was required to differentiate RID in natural kaolinites. The B center was removed by 250°C (2 h) heating (Clozel *et al* 1994); the A center was observed to remain after 400°C (24 h) heating (Angel *et al* 1974; Muller *et al* 1992); and A′ seemed to be of intermediate stability (Muller *et al* 1992). In the present work, systematic isochronal and isothermal heating experiments are conducted to obtain a better understanding of the thermal behaviour of the various RID in kaolinite.

The isochronal annealing was carried out for 2 h at 25°–50°C intervals over the temperature range 100°–450°C, i.e., up to a temperature at which the dehydroxylation process could occur (Brindley and Lemaitre 1987). These experiments should define the thermal conditions for individualization of center spectra.

The isothermal annealing experiments were performed in air at 300, 350, 375, 400°C, over a period of 120 h. They are of special interest to define the lifetime of some centers which are expected to be stable over geological periods under the thermal regime of the Earth's surface. Such stable centers are of the highest relevance in tracing past irradiations. The stability of heating temperatures (±2°C) was monitored, using a thermocouple in contact with the sample meltingpot in a tubular furnace.

Sample orientation. EPR spectra of polycrystalline samples, such as kaolinite, result in the superimposition of absorption lines from randomly distributed micro-crystals. In order to obtain an accurate assignment of EPR signals, i.e., to state the orientation of the crystal field axis of centers with respect to the crystallographic axes of kaolinite, it is necessary to prepare oriented samples. The kaolinite usually forms platy particles with preferential development according to the (ab) crystallographic plane. An orientation parallel to the (ab) plane was achieved both by compression and by sedimentation, resulting in oriented-powder specimen. X-ray diffraction confirmed that both orientation methods were effective because only 001 reflexions were observed on diffraction patterns of oriented samples. It was also verified, through X-ray diffraction, that the compression did not induce structural modification of the kaolinite structure.

EPR spectroscopy. Electron paramagnetic resonance spectra of RID were observed at X- (~9.2 GHz) and the Q-band (~35 GHz) using a CSE 109 Varian spectrometer. A higher frequency gives a lower detection limit and increases the gap between the spin levels, thus allowing acquisition of better resolved spectra. This increase in resolution allows a particularly clear distinction between frequency-dependent transitions (i.e., fine structure and Zeeman transitions) and the hyperfine structure, i.e., the resonances resulting from the interaction of unpaired electron spin and nuclear spin (Calas 1988 and references therein).

The experimental parameters were the following: 100 kHz frequency, 3.2 G amplitude for the modulation field and a time constant ranging from 0.125 to 0.25 seconds. Saturation behaviour of RID spectra as a function of microwave power (X-band) was investigated in order to give possible conditions of spectrum individualization. At room temperature (300 K), no saturation occurred in the range investigated (0–200 mW). At low temperature (77 and 93 K), the maximum amplitude is observed around 40 mW. However, the RID spectra are too similar to isolate them by differential saturation. Satisfactory conditions of observation were achieved using 40 mW microwave power for X-band and 16 dcb for Q-band. Low temperature 93 K recording was provided using a nitrogen-flow device, cooled by liquid nitrogen. This resulted in strong enhancement of the RID spectral intensity with respect to the background spectrum due to residual superparamagnetic iron-oxides (Bonnin *et al* 1982) and of the hyperfine structure of B-center (Meads and Malden 1975; Muller and Calas 1989; Clozel *et al* 1994).

The observed EPR signals were labelled by their g values, g_{eff} being defined by the relation:

$$h\nu = g_{eff}\beta B$$

where B is the field at which resonance occurs, ν is the resonance frequency, β is the Bohr magneton, h is the Planck's constant, g is a tensor with the eigenvalues g_{xx}, g_{yy}, g_{zz}. g-values were calibrated by comparison with a DPPH standard ($g_{DPPH} = 2.0036$). The error on g-value measurements was estimated to be ±0.001. The accuracy on magnetic field values was $\Delta B = \pm 1$ G. For comparison, it was convenient to present (in the same figure) the X- and Q-band spectra. However, it must be pointed out that only the g-values can be compared, as the magnitude and the magnetic-field positions of the resonances are frequency-dependent.

The oriented samples were aligned using a goniometer in the spectrometer, Θ stands for the angle between the direction of the magnetic field vector B and the (ab) plane.

Concentrations of centers are referred to a constant filling-factor of the X-band resonance cavity. They are proportional to the number of spins per mg, expressed in arbitrary units (a.u.) corresponding to integrated absorbance per mg per unit of gain. Due to the similar nature of the three types of centers, i.e., oxygen hole centers (spin ½), and the close g-values and line-widths measured on their spectra, these arbitrary units are

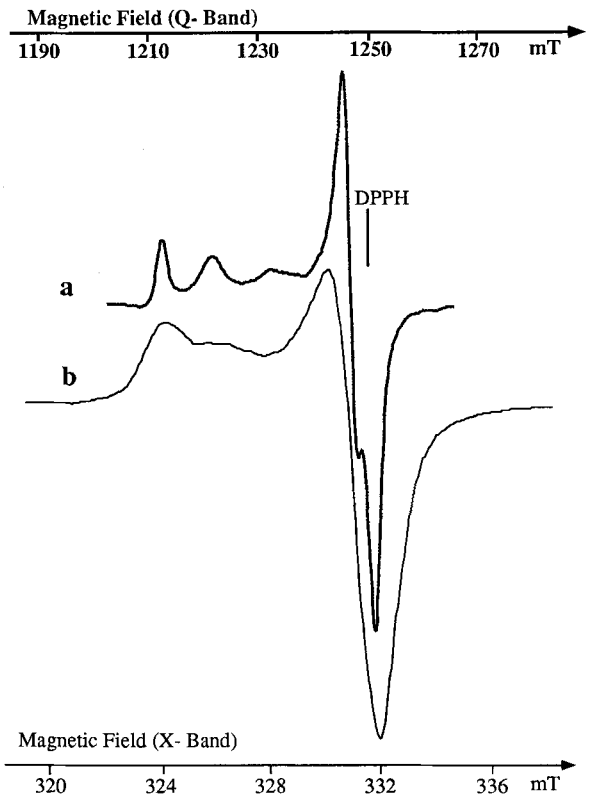

Figure 1. EPR signal (300 K) of radiation-induced defects in the natural kaolinite A1. (a) Q-band spectrum (b) X-band spectrum.

considered equivalent from one center to the other. Error on RID content determination was assumed to be within ±10%, taking into account additional errors on weighing and EPR recording. It should be noticed that Q-band setting is far less suitable for quantitative measurement, mainly because of the low reproducibility of sensitivity and substantial error arising from the weak mass of samples (a few mg).

Baseline corrections of EPR spectra. Strong baseline perturbations arose from the presence of iron oxides which are always associated with natural kaolinites (Malengreau *et al* 1994). These oxides are responsible for a broad resonance ($\Delta B > 1000$ G) which superimposes on the investigated EPR signal, whenever the oxides occur as distinct phases or as coatings (Angel and Vincent 1978; Bonnin *et al* 1982). Fe oxides have thus been eliminated prior to irradiation, using the complexing dithionite-citrate-bicarbonate (DCB) method (Mehra and Jackson 1960), which has no influence on the kaolinite structure nor the shape and the intensity of the RID spectra (Muller and Calas 1989). However, the iron oxides cannot be removed totally, particularly in soil samples (Herbillon *et al* 1976; Muller and Calas 1989). A weak broad isotropic resonance remained due to residual nanocrystalline, superparamagnetic iron oxide species (Muller and Calas 1993), whenever its intensity was reduced at low temperature. In most cases, the resonance due to remaining Fe-oxides was negligible with respect to the RID signal so that it could be approximated by a straight line. In some samples, such as BAR, this procedure can not be applied because of a relatively strong absorption due to remaining Fe-oxides. The contribution of the latter was thus approached by using the Fe-oxide signal from deferrated saprolitic kaolinites from Brazilian laterites, which were shown to be relatively intense with respect to that of RID (Muller *et al* 1992).

RESULTS AND DISCUSSION

Nature of the radiation-induced defects

RID ($g_{eff} = 2$) resonances are expected to occur near 1280 mT at Q-band, superimposed on a predicted signal involving Fe^{3+} (Meads and Malden 1975). Figure 1a shows an expanded version of a representative Q-band spectrum of RID in the range 1190 mT to 1280 mT. In comparison, the corresponding more familiar (see references above) X-band spectrum of RID, which is known to occur in the range 320 mT to 336 mT, is shown on Figure 1b. It is clear that the Q-band spectrum is more complex than the one at X-band, as expected from former results of the superimposition of well resolved signals with different shape and intensity. Further information about the different contributions were obtained on Q-band spectra of irradiated and annealed kaolinite samples.

Evidence for one type of Al-O^--Al center (B-center). All the X-ray irradiated kaolinites exhibited a Q-band spectrum presenting an orthorhombic anisotropy with narrow hyperfine multiplets on the three components of the signal (Figure 2a). The corresponding X-band spectrum (Figure 2b) is similar to that of irradiated synthetic kaolinite (Angel *et al* 1974). It reveals, particularly, the presence of a hyperfine pattern containing a total of nineteen lines, the position and the spacing (about 0.8 mT) of which were measured on EPR spectra of natural kaolinites recorded at low-temperature (Meads and Malden 1975). It must be pointed out that the shape of these spectra is not affected by subtraction of spectra obtained after annealing experiments.

The hyperfine structure was recently extracted from the bulk Q-band spectra of two well-crystallized kaolinites, among which was the GB3 sample, thanks to an appropriate convolution of the signal by a normalized square function (Clozel 1991; Clozel *et al* 1994). Three clearly separated multiplets of 11 equidistant (0.76 mT) hyperfine lines centered at $g_1 = 2.040 \pm 0.0005$, $g_2 = 2.020 \pm 0.0005$ and $g_3 = 2.002 \pm 0.001$ and exhibiting intensities according to the approximate ratio 1:2:3:4:5:6:5:4:3:2:1 were apparent. The hyperfine pattern was assigned to the interaction of an unpaired electron ($S = ½$) with two adjacent nuclei ^{27}Al

https://doi.org/10.1346/CCMN.1994.0420601 Published online by Cambridge University Press

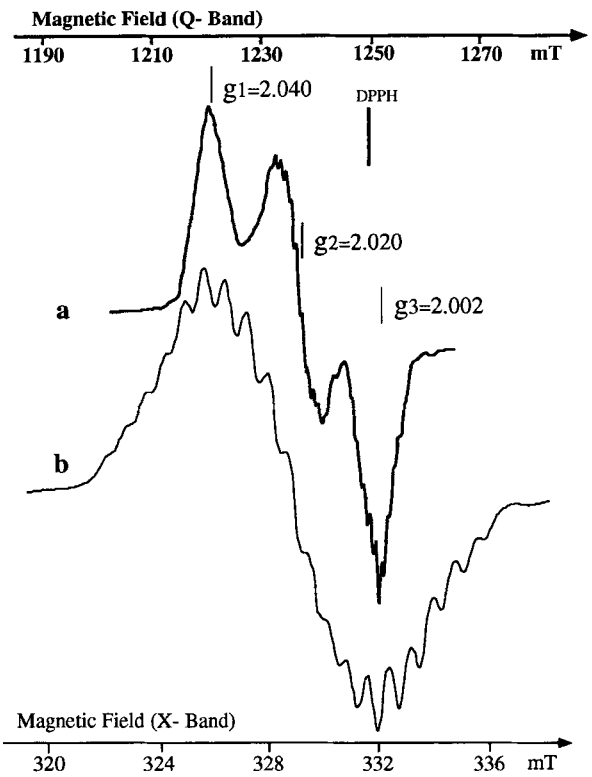

Figure 2. EPR signal of the B-center (77 K), sample GB3 (a) Q-band spectrum exhibits the orthorhombic symmetry of g tensor. The superhyperfine structure consists of three multiplets centered on the g_1, g_2, g_3 components (b) X-band spectrum shows an apparent cubic symmetry, because of the overlapping of the superhyperfine components.

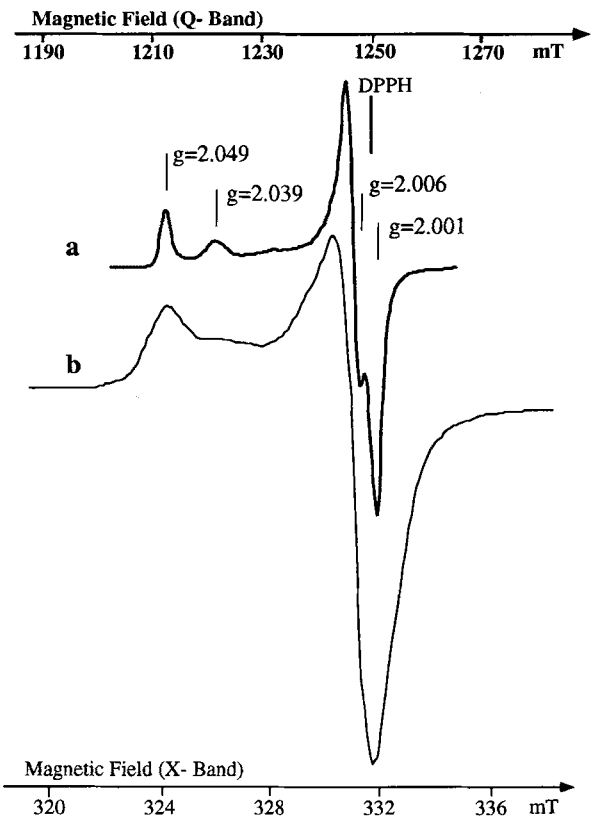

Figure 3. Annealing of the B-center. Several anisotropic resonances remain, which can be distinguished by further heating.

(I = 5/2; natural isotopic abundance = 100%) that are equidistant from the paramagnetic center. The apparent 19 line pattern frequently observed on X-band spectra of natural kaolinites was interpreted as resulting from the overlapping of these super hyperfine (SHF) structure lines. The anisotropic components at $g^{1,}$ g_2, and g_3 are correlated to the corresponding SHF multiplets, thus only one type of center is responsible for the observed spectrum, labelled B-center after Angel *et al* (1974). The various structural alternatives considered by Clozel *et al* (1994) led to the reasonable conclusion that this center is a hole trapped on the oxygen bonding two Al in adjacent octahedral positions (Al_{VI}-O^--Al_{VI} bridge). Thus, the previous assumptions from Angel *et al* (1974) and Meads and Malden (1975) that one or two centers are located on oxygen bonding Al in a tetrahedral position are no longer considered valid.

Evidence for two types of Si-O⁻ centers. As shown on Figures 3a and 3b, B-centers can be completely annealed equally well in irradiated as in natural samples by heating at a temperature ranging from 250°C to 300°C for a few hours. This is apparently due to the total disappearance of the superhyperfine structure and of the main component of the B-center centered at g_2 = 2.020. At the same time, it is observed that: (1) the B-center component centered at g_1 = 2.040 is replaced by a weak feature centered at g = 2.039 ± 0.0005; (2) the B-center component centered at g_3 = 2.002 is replaced by a doublet of sharp, intense resonances at about the same g-value; and (3) a relatively sharp resonance is present at g = 2.049 ± 0.0005. A progressive increase in temperature results in a continuous decrease of the intensity of the resonance at g = 2.039, which completely disappears at 400°C, while the intensity of the resonance at g = 2.049 remains quite unchanged (Figure 4a). Moreover, at 400°C, the lines from the sharp doublet around g = 2.002 are better resolved. By increasing the heating up to 450°C for 20 hours, a slight decrease of the intensity of the three remaining resonances at g = 2.049 and around g = 2.002 is observed. This allows the identification of one center spectrum.

This center is stable at elevated temperatures, up to 450°C. Its EPR spectrum presents a weak orthorhombic symmetry with the following g-values: g_z = 2.0490 ± 0.0005, g_y = 2.006 ± 0.001, and g_x = 2.001 ± 0.001 (Figure 4a) in agreement with data obtained on soil

https://doi.org/10.1346/CCMN.1994.0420601 Published online by Cambridge University Press

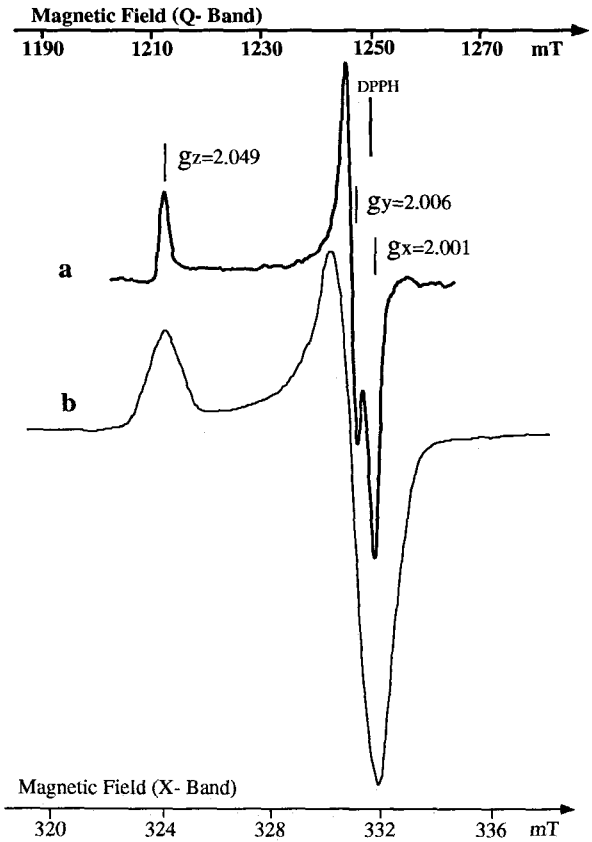

Figure 4. EPR signal of the A-center, sample A1. (a) Q-band spectrum, the center presents an orthorhombic symmetry (b) X-band spectrum shows an apparent axial symmetry, because g_y and g_z components are too close to be resolved.

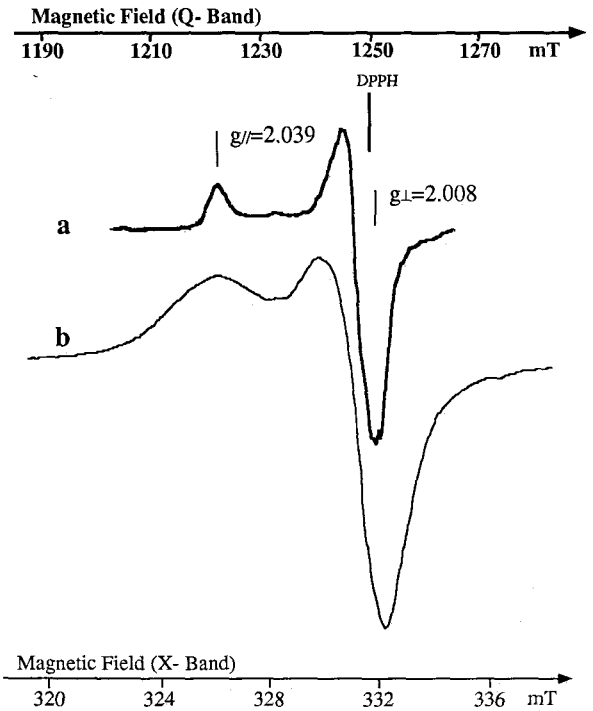

Figure 5. EPR signal of the A'-center, sample A1. Spectra are individualized by subtracting the suitable amount of A signal from the signal of Figure 3. (a) Q-band spectrum (b) X-band spectrum.

kaolinites (Muller 1988). The X-band spectrum (Figure 4b) only exhibits a doublet, which suggests an apparent axial symmetry of the g tensor ($g// = 2.049 \pm 0.002$ and $g\perp = 2.007 \pm 0.001$), since the g_y and g_x components are too close to be separated. These values characterize unambiguously the ubiquitous A-center (Angel *et al* 1974; Muller and Calas 1989; Clozel 1991). The A-centers have been interpreted as holes trapped on an apical oxygen atom. They have been noted Si-O^--centers by reference to the Marfunin's systematics (Marfunin 1979). The Q-band orientation dependance demonstrates that the g_z component is oriented perpendicular to the (ab) plane (Figure 6), as stated previously from X-band spectra by Jones *et al* (1974). While the g-values for A-centers remain constant in natural kaolinites, the half-width of the g// component varies slightly among the samples within 0.7–1.3 mT. It was shown earlier that these variations are closely related to the structural order of the sample, i.e., the thickness of coherent domains assessed by width at half-height of the (002) X-ray diffraction line. The wider the g// component, the smaller the coherent domain (Clozel 1991). A precursor model for the A-center was proposed by Angel *et al* (1974), which involved a divalent ion (Fe^{2+} or Mg^{2+}) substituted for Al^{3+} in the octahedral sheet. This model was supported by experimental evidence, and it explains the high stability of the center by local charge unbalance compensation.

The unexplained resonance in Figure 3 (g = 2.039) exhibits a thermal stability intermediate between those of B- and A-center spectra. The relevant signal can only be isolated by subtracting the suitable portion of the A-center spectrum from that of Figure 3, this portion being deduced from the intensity of its parallel component. The resulting asymmetric doublet (Figure 5a) characterizes a center of axial symmetry (S = ½) with EPR parameters ($g// = 2.039 \pm 0.002$ and $g\perp = 2.008 \pm 0.001$) that are distinct from those of the A-center. These values are also confirmed on the X-band spectra obtained with the same subtraction procedure (Figure 5b). They are those reported for the so-called A'-center identified by Muller *et al* (1990). The g-values are higher than those of the free electron (g = 2.0023), so these centers likely originate from trapped holes (Marfunin 1979). As the corresponding resonances are devoid of apparent hyperfine structure at liquid nitrogen temperature, this center was considered as a second type of Si-O^--center. It must be also pointed out that the half-width at half height of the g// component of the A'-center is higher than that of the A-center (e.g., on the sample C14, 12 G for A' and 8

https://doi.org/10.1346/CCMN.1994.0420601 Published online by Cambridge University Press

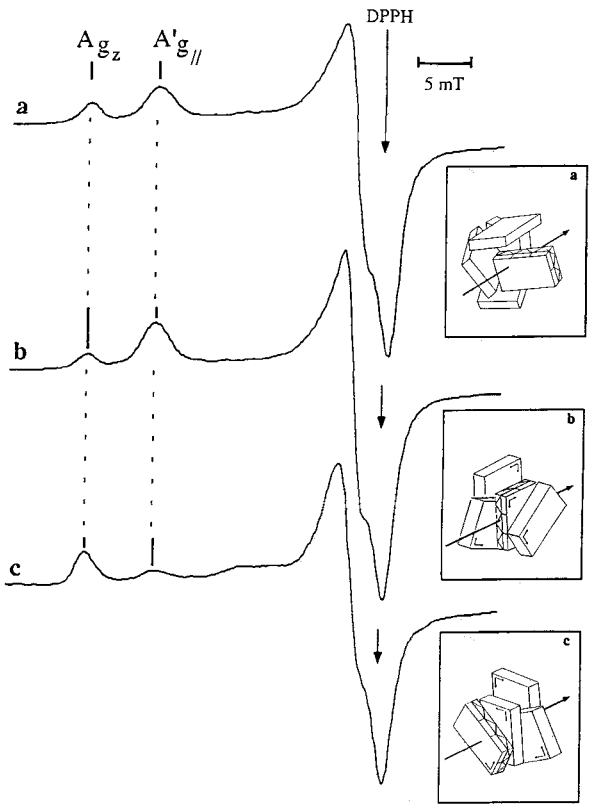

Figure 6. Orientation dependence of A′-center with respect to A-center (Q-band) (a) powder spectrum. The two centers are nearly orthogonal, as can be seen from oriented powders with B// (ab) plane (b) and B⊥ (ab) plane (c).

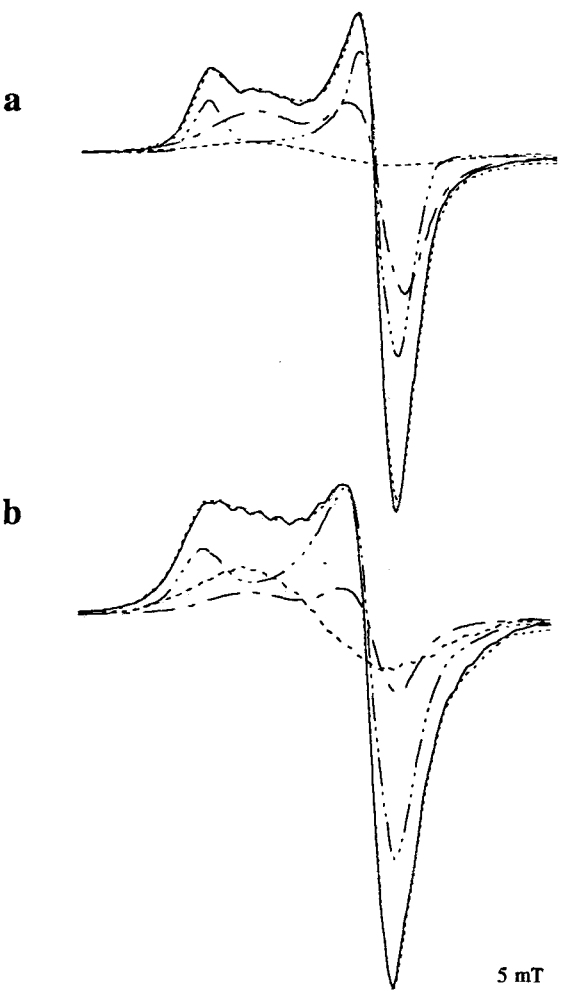

Figure 7. Least squares linear decomposition of the RID signal: —— Experimental; ····· Fit; —·····— A-center; —-— A′ center; – – – B-center (a) at 300 K for the kaolinite A1, (b) at 93 K for BAR kaolinite. The contents of the radiation induced defects are deduced from the proportion of the respective spectra.

G for A). After the annealing of the B-centers, orientation experiments were also carried out on sample C3, which presented the most intense A′ spectrum (Figure 6a). The orientation dependence is shown in Figure 6 for two different orientations of the crystallites with respect to the magnetic field B. It is clearly observed that the parallel component of A′-center is more intense when B is parallel to the (ab) plane ($\Theta = 0°$; Figure 6b), by contrast to the A-center which is almost perpendicular to the (ab) plane ($\Theta = 90°$; Figure 6c). No model has yet been proposed for this center because of the lack of experimental evidence. Nevertheless, the substantial relative enhancement of A′-center induced by heavy ion beam (Pb^{2+} implantation, Muller *et al* 1990; Clozel 1991) strongly suggests it is directly related to some intrinsic point defects as vacancies or interstitials rather than substitutions.

Concentration of the radiation-induced defects

The content of the respective defects can be deduced from the quantitative contributions of the above-defined A, A′ and B spectra, using a least squares fitting procedure (linear decomposition). Due to the sample dependence of the A-center signal shape, it was necessary to anneal each kaolinite at 400°C for 24 hours in order to define their A-center spectrum. The reference spectrum for A′-center was that extracted from sample C3, the kaolinite from the Nopal U-deposit giving rise to the best identification of A′-center signature among all the natural kaolinites studied. The reference spectrum for B-center was that obtained with pre-annealed X-ray irradiated sample GB3.

The fitting procedure was tested on the X-band spectra of several kaolinites recorded at 300 K or 93 K, whatever the previous physical treatment (none, irradiation, heating). Figures 7a and 7b illustrate the results for well-ordered (A1) and poorly ordered (BAR) kaolinites, respectively. The EPR spectrum of sample BAR exhibits a relatively high contribution from Fe-oxide in the g = 2 region. As a consequence, it was baseline-

https://doi.org/10.1346/CCMN.1994.0420601 Published online by Cambridge University Press

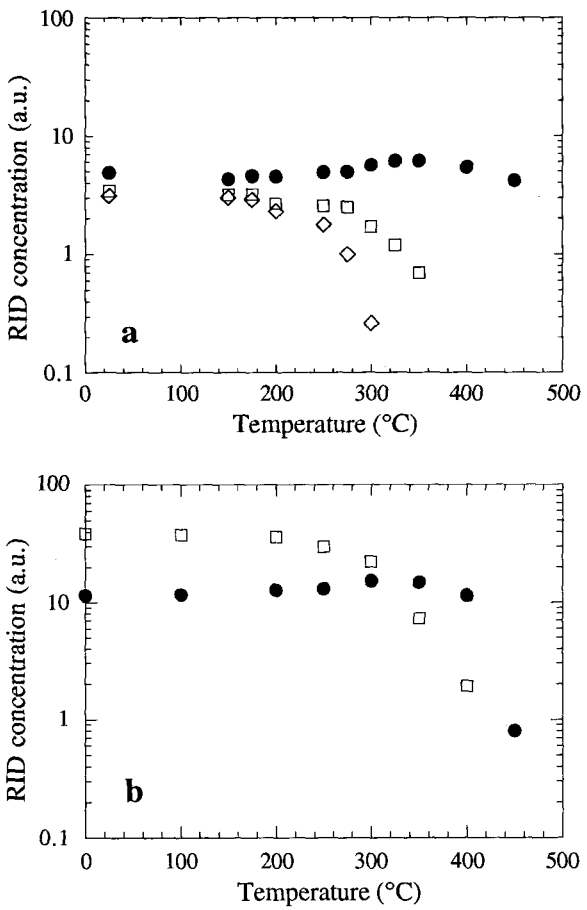

Figure 8. Isochronal annealing experiments: ● A-center; □ A′-center; ◇ B-center. (a) Kaolinite GB1, with similar initial contents of A, A′ and B centers (EPR recording at 93 K). (b) Kaolinite C3, characterized by high initial contents of A and A′ centers (300 K).

corrected (see "Methods" section) prior to linear decomposition. It can be observed that the fitted signals are in good agreement with the experimental ones. The RID spectrum of any natural kaolinite may be explained by the occurrence of the three types of hole centers described above. This confirmed the study of kaolinites from various environments by Clozel (1991). At the same time, this procedure allows the determination of center concentration in arbitrary units (the results obtained at 93 K for the natural kaolinites studied are given in Table 1).

Stability of the radiation-induced defects

The linear decomposition procedure (and the related quantification) allowed us to follow the behaviour of each RID during annealing experiments.

Isochronal heating. Isochronous annealing curves are illustrated in Figure 8 for two samples GB1 and C3, that contain substantially different amounts of defects (Table 1). Sample GB1 is characterized by about equal contents of A, A′ and B-centers. In contrast, the RID content is exceptionally high in C3, consisting of negligible B-, high A- and very high A′-center populations. It was verified that the thermal stability of the centers decreased in the order A-, A′-, B-centers over the temperature range 0–450°C.

The B-center is completely annealed over 300°C (2 h) heating, as can be observed at 93 K by its clearly resolved super hyperfine structure. Therefore, it can be inferred that the annealing temperature of B-centers in most samples is about 100°C higher than that reported in the literature (200°C; Angel *et al* 1974) depending on their initial concentration and temperature of the EPR recording.

The A′-center is stable up to 400°C (2 hours), as observed for sample C3. At this temperature it was no longer detectable in GB1 due to the lower initial content.

Finally, the A-center is stable up to 450°C, i.e., at a temperature close to that at which the dehydroxylation process occurs. An interesting observation was that the signal intensity of the A-center increased in the range 250–350°C and was restored at 400°C. This is evidenced by a maximum increase of about 30%, although data were fluctuated more for GB1. This behaviour suggested that some hole transfers occurred as a result of thermal activation. The source of this transfer was not clearly identified. It might be attributed to the A′-center decay, according to a constant relationship established between increase of the A-center and decrease of the A′-center content at 300 K measurements (Clozel 1991). Such electron transfers during annealing experiments have been reported in the literature for various materials (Griscom 1984; Hennig and Grün 1983). As this process would also happen at ambient temperature during geological time, it will have to be taken into account for the assessment of radiation dosage (paleodose) in the geosphere.

Isothermal heating. Temperature-dependent kinetics of decay were experimentally investigated by isothermal annealing, which allows the assessment of half-life, $t_{1/2}$, and activation energy, E_a (eV). The processes of decay are classically described by first or second order equations (Furetta 1988). The first order (Arrhenius) law can be written:

$$[A] = [A_0]e^{-Kt} \quad (3)$$

where [A] is the instantaneous defect concentration (a.u.), $[A_0]$ is the initial concentration, t is time of decay and K is the probability of decay per second, which can be expressed as:

$$K = (t_{1/2})^{-1} \text{ Ln } 2 = s_0 \cdot e^{-E_a/kT} \quad (4)$$

s_0 being the frequency factor usually in the range 10^8–10^{10} s^{-1} (Marfunin 1979), k the Boltzman constant (k

https://doi.org/10.1346/CCMN.1994.0420601 Published online by Cambridge University Press

$= 8.6\ 10^{-5}$ eV K^{-1}) and T the temperature (K). From relation (4) it can be seen that the half-life is only temperature dependent, and that at least two isotherm curves are required to determine E_a. These deductions are usually assumed in the fields of EPR or thermoluminescence (TL) dating, to assess the lifetime of RID. In various minerals investigated by TL, the ranges of activation energy and lifetime at 15°C were 1.6–1.9 eV and 10^6–10^{10} years, respectively (Aitken 1985). These are consistent with EPR data obtained for quartz (Shimokawa and Imaï 1987) or calcite (Hennig and Grün 1983; Wieser *et al* 1985).

Some more complex mechanisms may occur involving transit stage or retrapping in the decay process, which are described by a second order decay law of the form

$$[A]^{-1} = K \cdot t + [A_0]^{-1} \quad (5)$$

and

$$K = \text{tg}\ \theta = (t_{1/2} \cdot [A_0])^{-1} = s_0 \cdot e^{-E_a/kT} \quad (6)$$

or

$$\text{Ln}\ K = \text{Ln}\ s_0 - (E_a/k)T^{-1} \quad (7)$$

where θ is the slope of the linear curve (5). It should be noticed that the concept of half-life is temperature- and time-dependent (function of $[A_0]$). Values of K can be calculated at different temperatures from (5), and the constants E_a, s_0 by fitting the linear expression of T^{-1} in (7).

Both first and second order equations were used to describe the isothermal annealing of the A-center. Curves are plotted in Figure 9 for sample C14, the A-center content of which is exceptionally high. The best description of the data set was obtained with a second order relation, as evidenced in Figure 9a. Using results from 350°C, 375°C and 400°C annealing curves (Figure 9b), it was determined that E_a was 2.0 ± 0.1 eV and $t_{1/2} > 10^{13}$ years at 300 K for C14. Furthermore, the comparison of 400°C isotherms obtained on other samples led to the observation that the mean half-life seems to decrease with increasing disorder. This should be confirmed by more extensive study, as it is difficult to obtain reliable data below 400°C, for kaolinites with low defect content. For example, on sample BAR, it was possible to assume first order kinetics and likely values of s_0 between 10^8 and 10^{10} s^{-1}, leading to E_a in the range 1.8–2.1 eV, and a minimal half-life of 10^{12} years. Such mean half-lives are surprisingly greater than those reported for radiation hole-centers in other minerals. The stability of the A-center in kaolinite is considered to be sufficient to accumulate the natural radiation dose over geological time.

No systematic isothermal annealing was performed on A′- and B-centers. Nevertheless, assessment of the

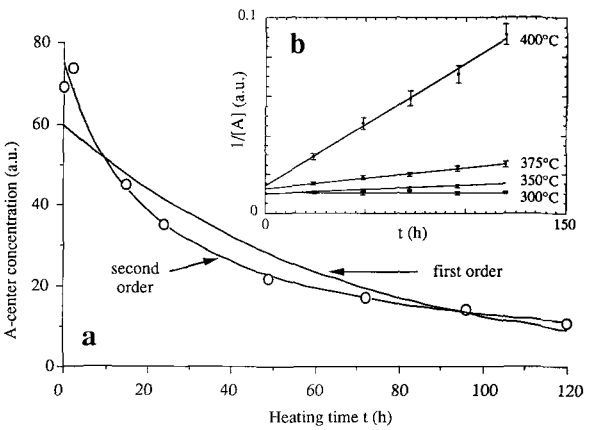

Figure 9. Isothermal annealing of the A-center in kaolinite C14 (open circles). The relevant EPR spectra were recorded at 300 K. (a) Linear representation of the 400°C isotherm: the decay law is described by second order kinetics. (b) On 1/[A] representation, the fitting of isotherms provides values of the temperature dependent decay constant K (h^{-1}), as the slope of the curves. The activation energy and the mean half-life are subsequently deduced from equation (7) in text.

half-lives at 300 K can be tentatively deduced from the above mentioned results, assuming that activation energies are in the range 1.6–1.9 eV: then, using data from the isochronal annealing, the magnitude of $t_{1/2}$ was calculated to be 10^2–10^3 years for A′-center and 10–10^2 years for B-center.

CONCLUSIONS

The observed Q-band EPR spectra of irradiated, annealed and oriented kaolinites from various origins, clearly show that only three types of radiation-induced defects, namely A-, A′- and B-centers, are present:

(1) A-center ($g_z = 2.0490 \pm 0.0005$, $g_y = 2.006 \pm 0.001$ and $g_x = 2.001 \pm 0.001$) is a $Si\text{-}O^-$ center with almost orthorhombic symmetry, with the z axis close to the c direction;

(2) A′-center ($g// = 2.039 \pm 0.002$ and $g\perp = 2.008 \pm 0.001$) is a $Si\text{-}O^-$ center with axial symmetry, its g// component being in the (ab) plane;

(3) B-center ($g_1 = 2.040 \pm 0.0005$, $g_2 = 2.020 \pm 0.0005$ and $g_3 = 2.002 \pm 0.001$) is a hole trapped on the oxygen bonding Al in adjacent octahedral positions (Al_{VI}-O^--Al_{VI} bridge).

The respective content of A-, A′- and B-centers can be determined in any natural kaolinite from a least squares fitting of the relevant EPR spectrum.

The thermal stability of the centers within 0–450°C decreases in the order $A \gg A' > B$, and their half-life values extended over a range of ten orders of magnitude. In particular, the activation energy and the mean half-life for A-centers, were $E_a = 2.0 \pm 0.2$ eV and $t_{1/2} > 10^{12}$ years, respectively. Such a mean half-life is sufficiently long to use kaolinite for radiation dosimetry under any thermal regime at the Earth's surface.

https://doi.org/10.1346/CCMN.1994.0420601 Published online by Cambridge University Press

ACKNOWLEDGMENTS

This work was supported by the Commissariat à l'Energie Atomique (DCC/DSD/SCS) and the PEGI (CNRS-INSU-ORSTOM) program. The authors are much obliged to G. Calas for fruitful discussions and to B. Morin (Centre de Spectrochimie, Université Paris 6) for technical assistance in EPR measurements.

REFERENCES

Aitken, M. J. 1985. *Thermoluminescence Dating.* London: Academic Press, 359 pp.

Angel, B. R., J. P. E. Jones, and P. L. Hall. 1974. Electron spin resonance studies of doped synthetic kaolinite I. *Clay Miner.* **10**: 247–255.

Angel, B. R., and W. E. J. Vincent. 1978. Electron spin resonance studies of iron oxides associated with the surface of kaolins. *Clays & Clay Miner.* **26**: 263–272.

Bonnin, D., S. Muller, and G. Calas. 1982. Le fer dans les kaolins. Etude par spectrométries RPE, Mössbauer, EXAFS. *Bull. Minéral.* **105**: 467–475.

Brindley, G. W., and J. Lemaitre. 1987. Thermal, oxidation and reduction reactions of clay minerals. In *Chemistry of Clays and Clay Minerals.* A. C. D. Newman, ed. Mineralogical Society Monograph 6. 319–364.

Calas, G. 1988. Electron paramagnetic resonance. In *Spectroscopic Methods in Mineralogy and Geology, Reviews in Mineralogy* **18**. F. C. Hawthorne, ed. Washington, D.C.: Mineralogical Society of America, 513–571.

Cases, J. M., O. Liétard, J. Yvon, and J. F. Delon. 1982. Etude des propriétés cristallographiques, morphologiques, superficielles de kaolinites désordonnées. *Bull. Minéral.* **105**: 439–455.

Clozel, B. 1991. Etude des défauts induits par irradiation dans les kaolinites. Approche expérimentale et implications géochimiques. Thesis, Univ. Paris 7, Paris, France, 156 pp.

Clozel, B., J-M. Gaite, and J-P. Muller. 1994. Al-O^--Al paramagnetic defects in kaolinite. *Phys. Chem. Miner.* (accepted).

Cuttler, A. H. 1980. The behaviour of a synthetic ^{57}Fe-doped kaolin; Mössbauer and electron paramagnetic resonance studies. *Clay Miner.* **15**: 429–444.

Furetta, C. 1988. New calculations concerning the fading of thermoluminescent materials. *Nucl. Tracks Radiat. Meas.* **14**: 3, 413–414.

Giese, R. F. 1988. Kaolin minerals. Structures and stabilities. In *Hydrous Phyllosilicates, Reviews in Mineralogy* **19**. S. W. Bailey, ed. Washington, D.C.: Mineralogical Society of America, 29–66.

Griscom, D. L. 1984. Characterization of three E'-center variants in X- and γ-irradiated high purity a-SiO2. *Nucl. Inst. Meth. Phys. Res.* B Vol 1, 481–488.

Hall, P. L. 1980. The application of electron spin resonance to studies of clay minerals. Isomorphous substitution and external surface properties. *Clay Miner.* **15**: 321–335.

Hennig, G. J., and R. Grün. 1983. ESR dating in quaternary geology. *Quat. Sci. Rev.* **2**: 157–238.

Herbillon, A., M. M. Mestdagh, L. Vielvoye, and E. G. Derouane. 1976. Iron in kaolinite with special reference to kaolinite from tropical soils. *Clay Miner.* **11**: 201–220.

Ildefonse, P., J. P. Muller, B. Clozel, and G. Calas. 1990. Study of two alteration systems as natural analogues for radionuclide release and migration. *Eng. Geol.* **29**: 413–439.

Ildefonse, P., J. P. Muller, B. Clozel, and G. Calas. 1991. Record of past contact between altered rocks and radioactive solutions through radiation-induced defects in kaolinite. *Mat. Res. Soc. Symp. Proc.* **212**: 749–756.

Jones, J. P. E., B. R. Angel, and P. L. Hall. 1974. Electron spin resonance studies of doped synthetic kaolinite II. *Clay Miner.* **10**: 257–269.

Liétard, O. 1977. Contribution à l'étude des propriétés physicochimiques, cristallographiques et morphologiques des kaolins. Thèse de doctorat en Sciences Physiques., Nancy, France, 345 pp.

Malengreau, N., J. P. Muller, and G. Calas. 1994. Fe-speciation in kaolins: A diffuse reflectance study. *Clays & Clay Miner.* **42**: (in press).

Marfunin, A. S. 1979. *Spectroscopy, Luminescence and Radiation Centers in Minerals.* Berlin, Heidelberg, New York: Springer Verlag, 352 pp.

Meads, R. E., and P. J. Malden. 1975. Electron spin resonance in natural kaolinites containing Fe^{3+} and other transition metal ions. *Clay Miner.* **10**: 313–345.

Mehra, O. P., and M. L. Jackson. 1960. Iron oxide removal from soils and clays by a dithionite-citrate system buffered with sodium carbonate. *Clays & Clay Miner.* **7**: 317–327.

Muller, J. P. 1988. Analyse pétrologique d'une formation latéritique meuble du Cameroun. Essai de traçage d'une différenciation supergène par les paragénèses minérales secondaires. *Travaux et Documents Microfichés* **50**. ORSTOM Paris, 664 pp.

Muller, J. P., and G. Bocquier. 1987. Textural and mineralogical relationships between ferruginous nodules and surrounding clayey matrices in a laterite from Cameroon. In *Proc. Intern. Clay Conf., Denver, 1985.* L. G. Schultz, H. van Olphen, and F. A. Mumpton, eds. Bloomington, Indiana: The Clay Minerals Society, 186–196.

Muller, J. P., and G. Calas. 1989. Tracing kaolinites through their defect centers; kaolinite paragenesis in a laterite (Cameroon). *Econ. Geol.* **84**: 694–707.

Muller, J-P, and G. Calas. 1993. Genetic significance of paramagnetic centers in kaolinites. In *Kaolin Genesis and Utilization.* M. Bundy, H. H. Murray, and C. Harvey, eds. Bloomington, Indiana: The Clay Minerals Society, Special Pub. 1., 261–289.

Muller, J. P., B. Clozel, P. Ildefonse, and G. Calas. 1992. Radiation-induced defects in kaolinites. An indirect assessment of radionuclides migration in the geosphere. *Appl. Geochem.* Supl. Issue **1**: 205–216.

Muller, J. P., P. Ildefonse, and G. Calas. 1990. Paramagnetic defect centers in hydrothermal kaolinite from an altered tuff in the Nopal uranium deposit, Chihuahua, Mexico. *Clays & Clay Miner.* **38**: 600–608.

Murray, H. H. 1988. Kaolin minerals: Their genesis and occurrences. In *Hydrous Phyllosilicates, Reviews in Mineralogy* **19**. S. W. Bailey, ed. Washington, D.C.: Mineralogical Society of America, 67–90.

Pinnavaia, T. J. 1981. Electron spin resonance studies of clay minerals. In *Advanced Techniques for Clay Minerals Analysis, Developments in Sedimentology* **34**. J. J. Fripiat, ed. Amsterdam: Elsevier, 139–161.

Shimokawa, K., and N. Imaï. 1987. Simultaneous determination of alteration and eruption ages of volcanic rocks by electron spin resonance. *Geochim. Cosmochim. Acta* **51**: 115–119.

Wieser, A., H. Y. Göksu, and D. F. Regulla. 1985. Characteristics of gamma-induced ESR spectra in various calcites. *Nucl. Tracks Radiat. Meas.* **10**: 4/6, 831–836.

(Received 8 February 1994; accepted 1 June 1994; Ms. 2465)